Published in final edited form as:
Chem Res Toxicol. 2009 July ; 22(7): 1264–1276. doi:10.1021/tx9000754.

Non-linear cancer response at ultra-low dose: A 40,800-animal ED_{001} tumor and biomarker study

George S. Bailey[*,Φ,†,‡,§], **Ashok P. Reddy**[Φ], **Clifford B. Pereira**[§,¶], **Ulrich Harttig**[Φ], **William Baird**[Φ,§], **Jan M. Spitsbergen**[†], **Jerry D. Hendricks**[Φ,†,§], **Gayle A. Orner**[†,‡], **David E. Williams**[Φ,†,‡,§], and **James A. Swenberg**[II]

[Φ]Department of Environmental and Molecular Toxicology, Oregon State University, Corvallis, Oregon, USA, 97331

[†]Marine and Freshwater Biomedical Sciences Center, Oregon State University, Corvallis, Oregon, USA, 97331

[‡]Linus Pauling Institute, Oregon State University, Corvallis, Oregon, USA, 97331

[§]Environmental Health Sciences Center, Oregon State University, Corvallis, Oregon, USA, 97331

[¶]Department of Statistics, Oregon State University, Corvallis, Oregon, USA, 97331

[II]University of North Carolina at Chapel Hill, Chapel Hill, North Carolina, USA 27599

Abstract

Assessment of human cancer risk from animal carcinogen studies is severely limited by inadequate experimental data at environmentally relevant exposures, and procedures requiring modeled extrapolations many orders of magnitude below observable data. We used rainbow trout, an animal model well suited to ultra low-dose carcinogenesis research, to explore dose-response down to a targeted 10 excess liver tumors per 10,000 animals (ED_{001}). A total of 40,800 trout were fed 0–225 ppm dibenzo[*a,l*]pyrene (DBP) for four weeks, sampled for biomarker analyses, and returned to control diet for nine months prior to gross and histologic examination. Suspect tumors were confirmed by pathology, and resulting incidences were modeled and compared to the default EPA LED_{10} linear extrapolation method. The study provided observed incidence data down to two above-background liver tumors per 10,000 animals at lowest dose (that is, an un-modeled ED_{0002} measurement). Among nine statistical models explored, three were determined to fit the liver data well - linear probit, quadratic logit, and Ryzin-Rai. None of these fitted models is compatible with the LED_{10} default assumption, and all fell increasingly below the default extrapolation with decreasing DBP dose. Low-dose tumor response was also not predictable from hepatic DBP-DNA adduct biomarkers, which accumulated as a power function of dose (adducts = 100 * $DBP^{1.31}$). Two-order extrapolations below the modeled tumor data predicted DBP doses producing one excess cancer per million individuals ($ED_{10}{}^{-6}$) that were 500–1500-fold higher than that predicted by the five-order LED_{10} extrapolation. These results are considered specific to the animal model, carcinogen, and protocol used. They provide the first experimental estimation in any model of the degree of conservatism that may exist for the EPA default linear assumption for a genotoxic carcinogen.

CORRESPONDING AUTHOR FOOTNOTE: Address correspondence to George S. Bailey, george.bailey@oregonstate.edu, Environmental and Molecular Toxicology Department, Oregon State University, Corvallis, OR, 97331; Phone: 541-737-3164; Fax: 541-737-5077.
Current affiliations are Department of Microbiology, Oregon State University (JMS); Proteogenix, Inc. Beaverton, OR 97006; Dept. of Epidemiology (APR), German Institute of Human Nutrition Potsdam-Rehbruecke Nuthetal, Germany (UH).

Supporting Information Available: The full tumor dataset (on a per-tank basis) is available in the supporting information section.

Keywords

dibenzo[*a*,*l*]pyrene; cancer risk assessment; dose-response; non-linear; ED_{001}

Introduction

Assessment of human cancer risk from environmental carcinogen exposures remains a challenging and inexact prospect. According to the March 29, 2005 *Guidelines for Carcinogen Risk Assessment* (www.epa.gov/cancerguidelines), cancer risk is estimated using a human case-specific dose-response model, if such a model is available (1). In this instance, the effective exposure leading to a specified level of risk may be interpolated directly from the dose-response curve. Alternatively, sufficient information on mode of action and critical parameters may allow development of a biologically-based model to be used in dose-risk characterization on an agent-specific basis. In the absence of either such model, dose-response risk evaluations are derived through extrapolation of experimental animal data from a high dose-response region, which has been measured experimentally, to a low dose-response region of interest, which has not been measured. The uncertainties introduced by these extrapolations remains a point of major concern. According to the 1996 Risk Assessment Workshop overview, "The major problem in cancer risk assessment [will] continue to be the inadequacy of available [low-dose] data on which to conduct more risk assessments."

The magnitude of the problem is outlined in Figure 1. Owing to costs and other limitations, dose-response data from a typical rodent carcinogen bioassay study are generally derived from a few hundred experimental animals, and thus are statistically limited to observations covering only about one order of magnitude, between 10% and 100% incidence. The EPA conservative approach models these high-incidence data to estimate the effective dose of that carcinogen to achieve 10% incidence (ED_{10}), and to generate a lower confidence limit on this dose estimate (LED_{10}) as a conservative point of departure for risk extrapolation. If the carcinogen is non-genotoxic or otherwise expected to produce a non-linear response, a Margin of Exposure procedure is applied to assign an acceptable human exposure. For genotoxic carcinogens, the conservative default assumption is that carcinogen-related cancer risk will extrapolate linearly toward zero exposure, that is, will vary in direct proportion to dose, below the LED_{10} estimate. Risk assessments based on this procedure can involve extrapolations several orders of magnitude below the actual experimental data. For example, estimation of the lifetime dose leading to one exposure-related (i.e. above-background) cancer case per million individuals (ED_{10}^{-6}) would require extrapolation to five orders of magnitude below the experimentally derived LED_{10} estimate (Figure 1).

Although there have been two previous large-scale rodent studies that might address this need (2–4), neither study provided treatment-related tumor data below 1% incidence. In any such low-incidence study, the lower limits for examining carcinogen-related, or background-corrected tumor risk will be bounded by several factors, among the most important being background target organ cancer rate. Hence the use of as many as 4080 animals in the BIBRA study (3) to examine N-nitrosodiethylamine (DEN) dose-response for hepatocarcinogenicity in Colworth rats provided insufficient statistical power to examine carcinogen-related tumor response below 5% because that is the approximate background cancer rate for that organ in that rat strain. The potential for large-scale studies is also severely limited by financial constraints (animal purchase and husbandry costs, carcinogen cost and availability, pathology costs) and a need for dedicated infrastructures capable of housing many thousands of individuals simultaneously.

We are investigating the feasibility of providing experimental carcinogen dose-tumor response data extending substantially below the 5% or 1% levels, using a well-established aquatic animal carcinogenesis model that circumvents many of these limitations. The species used in this study, the rainbow trout (*Oncorhyncus mykiss*), has historic background liver and stomach cancer rates near 0.1% in our facility, can be reared in the tens of thousands at extraordinarily low per diem and personnel costs, requires an infrastructure far less complex and of modest size compared to rodent requirements, and has well established pathologies and protocols for carcinogenesis experimentation (5–7). Based on these attributes, we have designed and completed the first of two four-part studies to determine if the rainbow trout would be capable of providing robust cancer dose-response data extending down to or below its historical background rate of 0.1% in liver.

Much attention also has been given to the possibility that readily quantifiable biomarkers of cancer risk, such as initial target organ carcinogen-DNA adduction (8–10), might provide accessible measures of eventual tumor outcome at exposure levels below those that can yield routinely measurable tumor response, with protocols requiring less time, cost, and infrastructure than an equivalent tumorigenesis bioassay. An obvious limitation to this approach, however, is the need for at least some experimental data to validate or assess biomarker-tumor dose-response correlations, down to measured ultra-low tumor response levels. We have incorporated one such biomarker assessment, qualitative and quantitative target organ DBP-DNA adduct measurements, into our study design to explore low-incidence biomarker correlations. We also assessed the adduction and tumorigenesis properties of several putative DBP intermediary metabolites, cell proliferation during exposure, and oncogenic Ki-ras mutational profiles in tumors at the end of the bioassay period to better understand dose-related mechanisms of tumorigenesis in this model.

DBP was selected as the test compound for this ED_{001} study due to its potency and widespread distribution in the environment. DBP is considered to be the most powerful naturally occurring carcinogen of the polycyclic aromatic hydrocarbon (PAH) class when tested in animal models of cancer (11,12). It is effective in multiple species (rat, mouse, trout, medaka), elicits tumors in multiple target organs (mammary gland, skin, liver, lymphoid system, lung in rodents; liver, stomach, swim-bladder in fish), and produces tumors via several routes of exposure (dietary, dermal, i.p. injection, transplacental) (11–16). DBP is found in the environment in particulates formed by combustion of smoky coal (17), in soil and sediment samples (18), and in cigarette smoke condensate (19). The human cancer risk posed by this potent genotoxic compound remains to be established.

Experimental Procedures

Materials

Dibenzo[*a*,*l*]pyrene (DBP ≥ 98% by HPLC) was obtained from the National Cancer Institute (NCI) Chemical Carcinogen Reference Standard Repository (Chemsyn Laboratories, Lenexa, KS, USA). This potent carcinogen was handled and stored in full compliance with Oregon State University (OSU) and NIH Guidelines for the use of Class C carcinogens. The semi-purified Oregon Test Diet (OTD) was prepared as described previously (20), except that menhaden oil (National Marine Fisheries Service, Charleston, SC, USA) was substituted for salmon oil. DBP was incorporated into the OTD at the stated concentration on a dry ingredients basis. Every batch of diet was assayed for DBP content, and results published elsewhere (21). The DBP dihydrodiols and dihydrodiol epoxides used in the embryo microinjection study were a generous gift of Albecht Seidel (Biochemisches Institute fur Umweltcarcinogene, Grosshansdorf, Germany).

Animals and exposure conditions

Shasta strain rainbow trout (*Oncorhynchus mykiss*) were hatched and reared at the OSU Sinnhuber Aquatic Research Laboratory (SARL) under previously detailed procedures (6, 20). All animal protocols were in accordance with NIH Guidelines and approved by the OSU Institutional Animal Care and Use Committee (IACUC). For each of four independent dose-response experiments, trout fry (initial weight 1.5 grams) were randomly assigned to 102 replicate tanks of 100 individuals each, and fed standardized OTD (20) until commencement of carcinogen treatment. Trout fry were then fed ODT only, or one of seven levels of DBP incorporated into OTD, for 4 weeks (Table 1). Each quartile included one sentinel tank of 100 fish in each of the eight exposure groups, to provide for biomarker sampling without disturbing fish density-growth interactions among tanks used for tumor determination. On days 15 and 29, 50 fish per dose per time point were sampled from these tanks for analysis of cell proliferation and DNA adducts. Following DBP treatment all remaining fish were fed OTD for the duration of the study.

Trout at each treatment dose were terminated beginning nine months later, under a gross necropsy protocol requiring 28 days to complete for each of the four replicate studies. Possible growth and time effects on tumor outcome were controlled by reduction of feeding to a minimal-growth maintenance schedule, and use of a random numbers routine assuring an average date of necropsy on day 15 among the replicate tanks at each carcinogen dose. By this strategy, there were no significant differences in tumor incidences among groups necropsied before and after day 15 (data not shown).

Histopathology

At necropsy, trout were deeply anesthetized in tricaine methane sulfonate, weighed, and the gill arches cut to allow bleeding. The liver, stomach, and swim bladder were removed from each fish and examined by a pathologist (JDH) with a dissecting microscope to detect gross tumors. We note that stomach and swim bladder tumors in the trout are readily detectable on the surface of the organs, and over 95% of liver tumors also appear on the surface. Suspect tumor locations were marked on livers and notes taken in order to successfully retrieve all grossly observed tumors. The organs were fixed in Bouin's solution for up to a week. Livers were then cut into 1 mm slices in which any interior tumors show up distinctly as pale yellow spots against the darker mottled background of normal liver tissue. All tumors and questionable lesions from the control and low dose groups were embedded for histological confirmation, but sections were not made from every liver in these groups if neither gross nor hand-slicing observation revealed any lesions. At higher doses, a single slide, having one or more tumors, was made from each tumor-bearing liver. With this protocol liver tumor incidence was histologically verified, whereas tumor multiplicity (not reported) above 1.0 might include some unconfirmed lesions. Sections were routinely stained with hematoxylin and eosin and established criteria for classification of trout liver tumors (6,22) applied. All pathological confirmation was by a single pathologist (JMS). Among the total of 1603 liver neoplasms identified in the study, the majority (71%) were hepatocellular carcinoma, 17% were mixed hepatocellular/cholangiocellular carcinoma, and 9.5% were hepatocellular adenoma. A few cholangiocellular carcinomas (1.5%), cholangiocellular adenomas (0.6%), and mixed adenomas (0.2%) were observed. Although a detailed morphometric study was not carried out, the observed spectrum of neoplasms was similar to this in all treatment groups and there was no apparent effect of DBP dose on the spectrum of observed tumor phenotypes. All stomach and swimbladder neoplasms examined were papillary adenomas. Whereas stomach adenopapillomas occurred frequently, only a few adenopapillomas were observed in the swim bladder among the thousands of animals examined. The response was too weak in this target to be of value in this investigation and is not further discussed.

DNA adduct analysis

DBP-DNA adducts in liver and stomach were examined using 3 pools of 5 samples each, taken from each sentinel tank of fish at days 15 and 29 of DBP treatment. Because trout liver appears largely deficient in global excision repair, bulky DNA adducts accumulate linearly with days of exposure and this time point thus approximates total cumulative DBP-DNA adduction in the target organ (23). DNA was purified and adducts initially characterized by ^{33}P-HPLC post labeling as well as ^{32}P-TLC post labeling, as described previously (14,24,25). Total hepatic DBP-DNA adducts were quantified for each treatment group using the more sensitive ^{32}P-TCL post-labeling method. Stomach DNA adducts were not quantified for this study.

Statistical Methods

Liver and stomach tumor incidence data were modeled as functions of the full range of DBP doses with the single exclusion of the highest dose (225 ppm) liver data due to the observed plateau of the liver tumor incidence as has been previously reported at this dose in the trout model (25). Standard error (SE) bars for pooled total (uncorrected) incidence (Figure 3B) are empirical based on observed variation between quartiles. The variation between replicate quartiles was found to be consistent with binomial variation at each dose modeled with the single exception of the liver data for DBP dose 28.4 ppm where there was considerable over-dispersion between replicate quartiles (11.6 times expected). SE bars for observed background-corrected incidence (Figure 4) are approximate and model-based (asymptotic likelihood-based assuming binomial variation at each dose for total (uncorrected) incidence with a variance-inflation factor of 11.6 included for the 28.4 ppm dose in liver tumor data only).

Nine models with independent background (extra risk) were initially fit to the total tumor incidence data. The Ryzin-Rai model (26) plus eight dichotomous models in the EPA Benchmark Dose Software (27) (gamma, Gompertz, Weibull, multistage, the two probit-type and the two logistic-type models) were all fit by maximum likelihood (assuming a conditionally binomial distribution) using the Nlmixed procedure in SAS version 9.2 (when allowing overdispersion at dose 28.4 ppm) and the EPA BMDS (27) software. Lack of fit was determined by likelihood ratio tests versus a saturated model with a parameter for every dose. Most models fit very poorly and only the three models that fit well are shown in the results. For liver tumor incidence data a quadratic term added to the logit linear in log dose model greatly improved the fit ($p=0.003$ likelihood ratio test for the quadratic term). Well-fitting linear (or quadratic) logit and probit models are linear (or quadratic) in log of DBP dose. The background incidence is small for both organs and, therefore, the results and conclusions are essentially the same whether one assumes independent background (extra risk) or additive background (added risk). Because the liver incidence pooled across quartiles at dose 28.4 ppm was highly consistent with the trend observed at neighboring doses, the conclusions regarding model lack of fit for liver data were the same whether or not the 28.4 ppm data were included in the modeling and, when it was included, whether or not a random quarter effect was added for the 28.4 ppm dose data.

LED_{10} values, using high-dose subsets of the observed liver and stomach data were obtained from the Probit procedure in SAS (inversecl option) using logit linear in log dose models and binomial variation (which meant that the over-dispersion of the liver incidence data at the DBP dose of 28.4 ppm would not be included and, therefore, would not penalize the LED_{10} approach by making it even more conservative). Hepatic DBP-DNA adduct accumulation data were log transformed and then modeled as a linear function of the log of DBP dose using the Reg and Glm procedures in SAS. The low-incidence log-log slope of the Ryzin-Rai model was compared to the adduct log-log slope with a Z-test assuming approximate normality and approximate independence of the two estimates.

Pathways to DBP-DNA adducts in trout

To investigate the metabolic origins of trout DBP-DNA adduction, trout embryos 27 days post-fertilization were microinjected with 1 μL of DMSO or 1 μL of DMSO containing either DBP (1, 10, 100, 1000 μg) or one of the following metabolites of DBP (250, 1000 ng): (+)-11,12-dihydrodiol, (−)-11,12-dihydrodiol, (+)-*syn*-11,12,dihydrodiol-13,14- epoxide, (−)-*anti*-11,12 dihydrodiol-13,14- epoxide and (±)-8,9-dihydrodiol. Two hundred embryos were injected per treatment group, with the injection directed into the yolk. The injected embryos were placed in incubation trays, hatched and reared to the sac-fry stage according to standard protocols. Three weeks days after hatching (22 days post-injection) and resorption of the yolk sac, two batches of 10 livers were taken from the survivors, immediately frozen in liquid nitrogen and stored at −80°C for adduct analysis. Remaining fish were fed OTD for 11 months, then sampled for tumors as described previously.

Cell proliferation analysis

Cell proliferation was assessed by proliferating cell nuclear antigen (PCNA) immunohistochemistry. PCNA was measured in livers and stomachs of 5 fish per dose per quartile sampled on days 15 and 29. Tissues were fixed for 24 hours in 10% neutral buffered formalin, then processed through a graded series of ethanols and xylene for embedding in paraffin. After processing and paraffin embedding, 4–5 μm sections were cut and mounted on charged slides, deparaffinized, and rehydrated in distilled water. The primary antibody was mouse anti-PCNA, PC10 (Dako, Carpinteria, CA), an antibody that has been validated for use in rainbow trout (23). The Dako Envision polymer system conjugated with peroxidase was used for the secondary antibody, and 3-amino-9-ethylcarbazole (AEC) was used as chromagen. Slides were counterstained with hematoxylin and mounted with Crystalmount (Biomeda Corporation, Foster City, CA). For each liver, 500 hepatocytes from each of two sections were counted (1000 per fish). For stomach, 500 surface epithelial cells and 500 glandular epithelial cells were counted per section (1000 of each cell-type per fish).

Detection of oncogenic Ki-ras

After digestion of tumor tissue with proteinase K, mutations in Ki-*ras* were analyzed by 3'-primer mismatch polymerase chain reaction (PCR) as described previously (28). Negative control DNA from livers of untreated animals gave PCR products only with the normal primers under these conditions. Positive mutations were verified by direct sequencing.

Results

Tumor dose-response data

The study design (see Table 1) used a protocol incorporating DBP into the standard OTD (5), to elicit tumors in trout liver and stomach. Two preliminary studies of 2000 animals each were conducted over a two-year period in order to select informative doses for the large-scaled experiment, and to permit model statistical calculations for optimal distribution of individuals along the dose range. A 30-year historic data base with the Shasta trout strain in our facility indicated a background liver cancer rate of approximately 0.1%, or 10 tumor-bearing animals per 10,000 individuals. Our aim in the final design was to elicit double this background incidence in liver at the lowest exposure dose (10 additional tumor-bearing animals per 10,000 trout) if the response remained approximately logit linear in log dose, as modeled for the higher dose pilot data, or a lesser number if it did not. The design called for 10,000 control animals (0 ppm DBP) distributed as 25 replicate tanks of 100 animals each for each quartile in the study, in order to provide a measure of true background and its variance. An additional 10,000 trout were similarly committed to estimate tumor response and variance at the lowest DBP exposure dose of 0.45 ppm. A further 18,000 animals were apportioned in decreasing number

with increasing dose and anticipated tumor response (Table 1). Dietary DBP doses covered a 500-fold exposure range, and were projected to provide liver tumor incidence data ranging from near background up to approximately 70% at the highest dose.

Of the initial 40,800 trout committed to the study design, 3200 were removed for early biomarker determinations and 32,316 were eventually sacrificed and the data utilized for tumor dose-response assessment (Table 1). Mean tank survival among these animal tanks was 92.4%, and deaths were unrelated to DBP dose. The remaining animals were lost from the study due to isolated malfunctions that disqualified 23 tanks from being considered. The protocol utilized a four-week carcinogen exposure period, after which animals were reared on control diet without DBP exposure for an additional nine months prior to sacrifice for histopathological examination. Logistics required that the study be carried out as four independent replicate experiments, each using one fourth of the animal total.

The observed total liver tumor incidences (background plus carcinogen-driven) for each of the four replicates are depicted in un-modeled, linear coordinates in Figure 2 (2A, entire incidence range; 2B, low incident range expanded). It is evident, especially in Figure 2A, that linear scales compress data in the most pertinent low dose region, and permit only a few general conclusions. The liver data set displayed a generally sigmoidal dose-response curve from above 60% to near zero, with independent replicates at each dose point falling within an absolute incidence range of 0.14 or less for the liver data (Table 1; Figure 2B). The measured pooled (mean) incidences were greater than control at all DBP doses, but not significantly so at either of the two lowest DBP doses, 0.45 and 1.27 ppm (Table 1). For six of the seven doses modeled (see below), the data are consistent with binomial variation between replicates (overall test for over-dispersion $p = 0.45$). The exception is the 28.4 ppm dose, where there is strong evidence of over-dispersion (deviance/df = 11.6, $p<0.0001$). Examining the pooled data (Fig 2B, solid line) at low range, as dose decreased the pooled line appeared curvilinear rather than straight as it approached background. Even without modeling, the observed extent of convex or “sublinear” behavior suggests that a low-incidence direct proportionality model would not fit the trout liver data, irrespective of background correction

Figure 2C shows the total tumor incidences in stomach for each of the four quartiles, also on linear coordinates. The four quartiles provided reproducible results, with the variation consistent with binomial variation at every dose (overall test for over-dispersion $p = 0.18$). DBP produced a less potent dose-response in stomach than in liver and did not approach the plateau observed at highest DBP dose in liver. The measured pooled incidences were greater than control at all DBP doses, but not significantly so at the three lowest doses of DBP (0.45, 1.27, 3.57 ppm). The background incidence in stomach was approximately 1.5 times that in liver (Table 1)

Although Figure 2 provides a useful overview of the focus and range of incidences observed in the two organs, it is clear from the data compression inherent in the linear-linear plot that a different scaling is necessary to more appropriately visualize low-dose, exposure-related tumor response at ultra-low incidence. Many scales are available. Waddell (29), for instance, recently reinterpreted the mouse 2-acetylaminofluorene (2-AAF) ED_{01} data using a scale linear in response (tumor incidence) but logarithmic in dosage (log 2-AAF molecules/kg/day). This scaling was, however, challenged on the basis of asymmetric data compression artifact (30). By comparison, a simple log-log plot of the trout data set (Figure 3) avoids data compression at low doses and provides a sensitive scaling for examining the EPA conservative default assumption that exposure-related response will vary in direct proportion to carcinogen exposure dose, without any ad hoc assumptions such as those inherent in semi-log scaling. On a log-log plot of background-corrected incidence vs. dose, low-incidence data consistent with

direct proportionality will appear as a straight line with slope not significantly different from 1.0, while a slope clearly greater than 1.0 will instead indicate sublinear behavior.

Model fitting to the tumor dose-response data

Figure 3A depicts the liver and stomach tumor incidence data sets without correction for observed background, which were 0.12% (95% binomial CI 0.056–0.21%) for liver and 0.18% (95% binomial CI 0.10–0.30%) for stomach. Figure 3B illustrates exposure-related (background-corrected) incidence vs. dose on the log-log. Though the variation in estimates of tumor incidences at the lower doses appear large on a log-log scale (e.g. Figure 2B, Figure 3A, 3B, Figure 4A), it must be noted that these in fact represent experimentally estimated frequencies of such very rare events as 1–2 tumors per 2000 individuals (Table 1). This is why four repeats, each consisting of as many as 25 replicates of 100 animals each were required to reasonably estimate response and its variance at low or zero dose. We note that low precision in estimating true background rate contributes strongly to the wide SE intervals for corrected incidences at the two lowest carcinogen doses and to the fact that the lower SE boundary includes zero for the corrected response in liver at the lowest dose (Figure 4A). Precision for background estimates has decreasing contribution to the SE intervals with increasing dose and observed incidence. These results illustrate that background tumor incidence in the model of choice is perhaps the limiting statistical factor in the design and interpretation of ultra-low dose-response studies.

The carcinogen-related (background corrected) tumor responses in liver and stomach are depicted in Figure 3B. The precise relationships between these responses and the LED_{10} default response were established by fitting models incorporating both background and dose response to the incidence data in Table 1 (see Statistical Methods). Figure 4A depicts the dose-response part of three well-fitting models, as well as an LED_{10} extrapolation derived solely from the higher dose/response region of the liver data set. We do not attach *a priori* any special biological significance to any of the three mathematical functions, but simply use them to explore the degree to which the experimentally measured tumor incidence data are compatible with the EPA default linear extrapolation. As seen in Figure 4, the three dose-response models (Ryzin-Rai, logit quadratic and probit linear) all fit the data extremely well ($p > 0.8$ for each lack of fit test respectively with 3, 3 and 4 df). In the well-fitting Ryzin-Rai model, there is a slope parameter that describes low-dose behavior. If that parameter is not clearly different from 1.0, then the estimated low-dose behavior is consistent with the EPA low-dose direct proportionality model. In fact, however, the Ryzin-Rai slope parameter is estimated as 2.278, with an asymptotic standard error of 0.356, demonstrating substantial sublinearity and strong evidence against direct proportionality at low dose ($p<0.0001$, likelihood ratio test that parameter = 1.0). The fitted logistic quadratic and linear probit models lack single slope parameters describing low-dose behavior, but instead show slopes that are even steeper than that for Ryzin-Rai, increasingly so with decreasing DBP dose (Figure 4A) Therefore, we can conclude that none of the three models that do fit the liver data well is compatible with the EPA default model, which would require that tumor response remain in direct proportion to carcinogen dose at low incidence.

A 5-log-order extrapolation of the default curve, using the LED_{10} estimate from the higher carcinogen doses only, estimates the dose expected to provide one excess cancer in a million individuals (ED_{10}^{-6}) to be 0.126 ppb DBP (Table 2). By comparison, the models fitted to the complete low-dose data set require only a two-order extrapolation to provide ED_{10}^{-6} estimates. These virtually safe dose estimates for liver range from 66 ppb (Ryzin-Rai) to 186 ppb (linear probit) DBP, doses that are 500–1500-fold greater (less hazardous) than predicted by the linear default procedure (Table 2).

We also explored fitting and extrapolation of the stomach tumor data set. An interesting possibility is that the attenuated response with decreasing dose in stomach reflects a hormetic, or J-shaped, dose-response in this organ (31). However, the suggestion of a J-shaped response curve rests solely on the single data point at lowest DBP dose, which is in fact statistically indistinguishable ($P < 0.5$) from the responses at zero and 1.27 ppm. The four models that were successfully explored were the LED_{10} linear extrapolation, Ryzin-Rai, linear probit, and linear logit (Figure 4B). In stomach there was greater variation at the four lowest DBP doses in both the data replicates and the fits of three models, compared with liver. These differences in target organ response assessments occur in large part because our choice of animal distributions for the study was optimized for liver, which had only two thirds the background incidence and a less steep DBP response compared with stomach. This is analogous to the less informative outcome that might result were an ED_{001} study undertaken without adequate preliminary dose-response data for the major (or only) target organ. As a consequence, model fits for the stomach data are determined chiefly by the high-dose data because the low-dose data are imprecise. Despite these limitations, we were able to conclude that the stomach data, like liver, are not compatible with the EPA default assumption. The logit linear in log dose model (3 parameters) fits the data well ($p = 0.336$, 5 df lack of fit test), as does a 3-parameter probit in log dose model ($p = 0.535$, 5df lack of fit test) and a 4-parameter Ryzin-Rai model ($p = 0.541$, 4 df lack of fit test). The slope estimates at low-dose for both the logistic linear model (1.97, SE 0.071) and Ryzin-Rai models (2.743, SE 0.454) are well above 1.0 indicating substantial sublinearity and strong evidence against direct proportionality ($p<0.0001$ likelihood ratio test that parameter=1.0). The slopes of the fitted curves were also extrapolated to estimate conservatism of the linear default model for this organ. These virtually safe dose estimates (linear logit, 0.12 ppm; Ryzin-Rai, 0.46 ppm; linear probit, 1.81 ppm) cover a greater range than for liver owing to the greater dispersion in the low-dose stomach data, and are 360 – 5500 times greater than the conservative LED_{10} 10^{-6} estimate of 0.00033 ppm DBP for cancer risk in stomach.

Biomarker results

Initial studies were conducted to resolve and quantify individual DBP-DNA adducts in the trout model, and to explore their metabolic origins (Figure 5–Figure 7.) HPLC resolution of ^{33}P-HPLC postlabeled adducts revealed three major adducts in stomach (Figure 5B), that partially overlapped with those generated by DBP metabolism in human MCF-7 cells (not shown). The major liver adducts were more numerous and much more polar than those in stomach (Figure 5A).

To explore metabolic origins, DBP and several potential metabolic intermediates (Figure 6) were microinjected into trout embryos at total doses up to 1000 ng/embryo, for determination of DNA adduct profiles and gross tumorigenicity. By this protocol, DBP elicited primarily liver-type adducts in total embryo DNA (Figure 7, upper panel), and a potent dose-response for hepatic tumor induction nine months later (Figure 7, lower panel). The synthetic (−)-11,12-dihydrodiol DBP derivative showed adduction and tumorgenicity similar to parent DBP. The (−)-*anti*-11,12-dihydrodiol-13,14-epoxide elicited primarily stomach-type DNA adducts, and a strong liver tumor response nine months later in liver. Interestingly, no stomach tumors were elicited by this DBP intermediate, which suggests that elements other than DBP adduct phenotype determine tumor organospecificity in this model. The (+)-*syn*-11,12-dihydrodiol-13,14-expoide showed similar but less extensive stomach-type adduction and liver tumor initiation. The DBP-(+/−)-7,8-dihydrodiol derivative induced no detectable adduction or tumorigenicity. We note that this experiment was not designed with sufficient replicates to establish an absolute carcinogenic potential of each DBP derivative by embryo microinjection. Further interpretation is also limited by the unusually high background liver cancer rate in this particular study.

Following these characterizations, total genomic DBP-DNA adducts were examined as potential biomarkers that might explain, or be used to predict, the shape of the tumor dose-response curve seen in trout liver. Figure 8A compares the un-modeled liver adduct and tumor incidence data sets at low DBP dose. This comparison suggests that use of adduct data as a surrogate for tumor data would be misleading here because the adduct data curve is less steep. This visual impression is born out by modeling results. As seen in Figure 8B, the adduct data set can be modeled successfully on a log-log plot as a straight line ($p=0.47$ lack of fit test) with a slope of 1.31 (SE 0.07). Although this indicates a significant ($p<0.0001$) sublinearity in adduct dose-response, it is a small degree of sublinearity compared to that observed in the modeling of the exposure-caused liver tumors. The Ryzin-Rai model gave a low-incidence slope of 2.28 (SE 0.036) on a log-log plot, a slope that is significantly greater than the 1.31 observed in the adduct model ($p=0.007$ two-sided approximate Z-test). Further, the other two well-fitting models indicate even steeper slopes (and therefore greater sublinearity) than that in the Ryzin-Rai model (Figure 4A). Therefore, use of liver DBP-DNA adducts as biomarkers to predict low-dose tumor response would have been misleading in this study. Specifically, adduct measurements, by being considerably less sublinear, would have suggested that the conservativeness of the LED_{10} extrapolation was much less than suggested by the actual tumor modeling (Fig. 4A).

It was important to know if non-concordance between adduct and tumor dose-response might be ascribed to dose-dependent changes in DBP metabolism that might alter the types, and hence the possible tumorigenic potencies, of DBP-DNA adducts formed. This was explored by examining the ^{33}P-HPLC profile of hepatic DBP-DNA adducts for dose-dependent changes. As expected, the absolute level of each HPLC adduct peak in liver was seen to increase with DBP dose (Figure 5C), however the ratio among adduct peaks did not appear to change with DBP dose. Hence non-concordance between adduct and tumor dose-responses are not due to dose-dependent alterations in the types of adducts formed by DBP.

We also investigated the effect of DBP dose on the proportion of proliferating cells in livers and stomachs of fish sampled at day 29, the end of carcinogen treatment. There was no evidence for an effect of DBP on PCNA staining among hepatocytes, stomach surface cells, and stomach glandular cells, except for a slight diminishment in liver at highest DBP dose (Figure 9). Therefore, while reduced proliferation might contribute to the plateau in hepatic tumor response at high DBP exposures, there is no evidence that this contributes to the diminishing response at low DBP levels. We did not explore markers of proliferation other than PCNA, or the potential role of dose-dependent apoptosis in this study.

Discussion

Data extrapolation, non-linearity, and risk characterization

The LED_{10} default model has, up until now, required extrapolation of measured animal data downwards through five orders of magnitude (100,000-fold below the modeled data set) to estimate the dose producing one excess cancer case in a million animals. The current dataset, however, extends down to an observed 0.02% liver tumor incidence and thus limits the need for extrapolation to less than three orders of magnitude beyond the lowest data point. Extrapolation through this greatly reduced range (200-fold below the modeled data set) by three different well-fitting models provides estimates of the virtual safe dose for liver that are 500 to 1500 times higher than that provided by the conservative LED_{10} extrapolation (Table 2). Similar results were obtained by modeling of the stomach tumor data. These findings in two different target organs provide the first case-specific experimental measures of the degree of conservatism that might exist for the default linear extrapolation method. A similar ED_{001} experiment is presently under way with aflatoxin B_1, the most potent known human dietary carcinogen, to expand our knowledge of carcinogen specificity in ultra-low dose-response.

DNA adducts as biomarkers of tumor dose-response

The present study examined two commonly considered biomarkers of effective carcinogen treatment, genomic DBP-DNA adducts accumulated during exposure, as well as Ki-ras oncogenic mutational profiles in tumors nine months after DBP treatment. Despite great progress in establishing relationships between carcinogen exposures, target organ carcinogen-DNA adducts, and tumor outcome, previous efforts have been unable to couple tumor with adduct data at ultra-low exposures and incidences. As a consequence, data have not been previously available to directly test the utility of DNA adducts as predictive biomarkers of tumor response at ultra-low incidence. We have shown here that the shapes of the initial carcinogen-DNA adduct dose- response and the eventual hepatic tumor response to carcinogen treatment can be distinctly different. Total genomic DBP-DNA adducts increased not linearly but as a power function of DBP dose, and thus modeled as a straight line with slope 1.31 (SE 0.061; 95% CI 1.19, 1.44) on a log-log scale. This DBP dose-adduct response behavior was significantly different from the DBP dose-tumor incidence response in liver. Two of the three models fitting the liver tumor data well, quadratic logit and linear probit, display increasingly steep slopes, and thus increasing departure from the DBP-DNA adduct line, with decreasing carcinogen dose. For these two models, there is no circumstance under which DBP-DNA adduction could be used to accurately predict tumor response at low exposure, or a virtually safe DBP dose. The third model, Ryzin-Rai, does approach linearity over the low dose-incidence range on the log-log scale (Figure 4A); however, the slope in this region is 2.28, not 1.31 ($p<0.007$). For this model as well, there is compelling evidence that measurements of genomic DBP-DNA adducts do not provide an accurate biomarker for ultra-low dose cancer risk evaluation.

The effect of these differences on risk evaluation are considerable. Figure 8A compares the shapes of the un-modeled adduct and incidence dose-response curves, normalized at the 10.1 ppm DBP dose point. If we use the fitted adduct function *log(adducts) = 2.000 + 1.31 log (DBP)* to predict the shape of a theoretical tumor dose-response curve below this 10.1 ppm DBP data point, as might be done in the absence of lower-dose tumor data, we obtain by extrapolation an ED_{10}^{-6} estimate of 2.5 ppb DBP. This estimate is 20-fold greater than that provided by the LED_{10} assumption, and thus leads to the conclusion that the LED_{10} assumption is conservative by a factor of 20 in this case. By comparison, ED_{10}^{-6} estimates obtained by extrapolation of the models fitted to the entire liver tumor data set were 500–1500 fold larger (less conservative) than the LED_{10}-derived ED_{10}^{-6} estimate (Table 2). Therefore, use of the adduct data in place of the more sublinear tumor data would lead to a 25- to 75-fold error in estimation of a virtually safe DBP dose, and a comparable difference in the assessment of LED_{10} conservatism, for this case-specific model.

Discordance between DNA adduction and tumor responses have been recognized for some time now with other carcinogens and animal models. For example, Poirier and Beland (32) found a non-correlation in BALB/C mice treated with 2-acetylaminofluorene between steady-state levels of DNA alkylation in bladder, which appeared to be linear, and bladder tumor incidence at 24 months, which was notably sub-linear. Driver et al. (33) reported a similar discordance between dimethynitrosamine-induced DNA adducts, which were depicted as a straight line plot on linear coordinates, and mesenchymal tumors, which showed a distinct sigmoidal dose-response on similar coordinates. In both studies, however, adduct-incidence correlations were restricted to the higher dose-response region (observed incidences above 0.3% or 1.25%, respectively) and not usable for ultra-low dose-response correlations. The latter study also suffered from absence of statistical treatments to support the claims.

Mutations as biomarkers of low-dose risk

A recent suggestion to incorporate more science into the risk assessment process involves developing high quality mutation dose response data in reporter genes that define the low dose mutagenic potential (8), followed by application of a reasonable safety factor to cover individual differences in metabolism and repair. Although carcinogen-driven DNA adducts provide important information on molecular dose at target tissues, cancer is considered to be a disease of mutations. DNA adducts are not mutations, and can induce mutations only with appropriate cell survival, adduct processing and fixation by replication. Perhaps under certain restricted conditions, cumulative carcinogen-DNA adducts might serve as predictive biomarkers of carcinogen-related (background-corrected) tumor response at ultra-low exposure, for instance where total adducts accumulate linearly with dose, the spectrum and the genomic distribution of adducts are independent of dose, adduct-driven oncogenic mutations remain in direct proportion to dose, and cellular homeostasis is independent of dose. This set of conditions appears not to be met in the present study.

Dose-dependent induction of CYP bioactivation, and/or saturation of limited DBP-DNA adduct repair capacity, are plausible mechanisms to explain the exponential dose-response behavior for genomic DBP-DNA adduction in trout, but can not account for lack of concordance between adduction and tumor induction. Alternative explanations might include non-linear dose-responses for adduction, repair, and/or mutagenesis at genes critical to tumor initiation, rather than genomic DNA. For instance, DBP adduct mutagenic potency may fall off with decreasing dose and adduct concentration, such that the low number of adducts present at ultra-low DBP doses might not drive oncogenic mutations above those from endogenous damage. We have at least partially explored this hypothesis by examining the frequency and spectrum of oncogenic Ki-ras mutations in liver and stomach tumors. Limitations of the approach include restrictions in the types and locations of oncogenic Ki-ras mutations recoverable from tumors, and in our study, a paucity of spontaneous and low-dose tumor fragments for examination (pathology took precedence, and Buoin's fixative precluded mutation examination in fixed tumor specimens). Despite these limitations, there is clear evidence from stomach tumors that DBP-driven mutations in the Ki-ras oncogene were present even at low dose. As seen in Table 3, the frequency distribution of oncogenic mutations in stomach tumors at the two lowest DBP doses (six of six codon 61 adenine based mutations) appeared to differ from those in tumors from the untreated control fish (three codon 12/13 guanine-based mutations, one codon 61 guanine-based mutation), and the differences became substantial at higher doses where the contribution of spontaneous tumors would be negligible (38 of 39 codon 61 adenine-based mutations). The probability that the spectrum of mutations in stomach tumors in controls and in tumors from the two lowest DBP doses should differ by chance alone, i.e. are not DBP based, is small ($p = 0.033$, Fisher's Exact Test). This result supports the idea that DBP-DNA adducts are contributing functioning, selectable mutations in genes critical for tumor development in this model, at least in one target organ, even at lowest DBP doses. It is intriguing that apparent DBP-driven mutations are detected even in the low-dose range where total tumor incidences in treated and control groups did not differ significantly. This may suggest that carcinogen treatment itself elicits an environment in which cells acquiring carcinogen-driven oncogenic mutations are selected over those carrying spontaneous mutations in the same oncogene. For liver, only three mutant alleles were detected among the five control tumors available for examination, and there was insufficient information to determine if a dose-related shift in mutant allele frequency may have occurred.

Protocol considerations

The current protocol assessed tumor response in a lower vertebrate tumor model. Non-mammalian status would present an obvious limitation if the present results, which provide an ED_{10}^{-6} risk evaluation for DBP in trout, were extrapolated directly to humans, or even to

rodents. We have suggested no such extrapolation. The goal instead was to provide an expanded experimental data set down to ultra-low exposures and incidences, to use these data for assessment of dose-linearity for tumor response, and to assess the utility of DNA adducts as biomarkers of tumor response at low dose. The results show clearly that the default extrapolation method for low exposure risk evaluation does not apply for this model, carcinogen, and protocol, and that adducts were not useful biomarkers for predicting eventual tumor outcome. While DBP carcinogenic potency may well differ in trout and humans, we have no basis to conclude that the fundamental shape of the DBP dose-tumor response curve would differ in these species.

It is also pertinent to consider the extent to which the deficiency in global repair of bulky DNA adducts seen in the trout model (23) relates to the observed shape of the tumor dose-response curve. One plausible expectation is that models with significantly decreased DNA repair capacity might have a greater tendency toward low-dose linearity than those with greater repair capacity, because they are less capable of adduct removal and mutation avoidance at ultra-low exposures. The fact that the current findings are not consistent with this expectation makes a low-dose-linearity response even less tenable than if the model had substantial DNA repair – that is, an animal with greater repair capacity would be expected to show an even steeper departure from linearity in the low-exposure region, not less. In this regard the trout provides a conservative measure of the conservatism in the LED_{10} default assumption.

A final consideration is that the present study relates most directly to risk characterization for juvenile cancer, which is second only to accidents as the leading cause of death among children in the US. The focus on juvenile risk is a direct consequence of our less-than-lifetime exposure protocol, which was necessitated by restrictions of the model (long life span, continued growth) as well as insufficiency of pure DB(a,l)P anywhere in the world to permit lifetime exposure in trout or any other vertebrate model. While juvenile cancer risk assessment is undeniably important, it is also pertinent to consider how data gathered from partial life exposure protocols may relate to the more traditional lifetime risk assessments. Based on our historical data, we would expect tumor incidence at any DBP dose to increase with time of treatment and time for tumor growth in the trout model. As a consequence, $ED_{10}{}^{-6}$ estimates from this model would be expected to increase with longer treatment or grow-out times. The more important question, however, is whether the fundamental shape of the dose-response (e.g. linear vs. non-linear) would be influenced by either parameter in trout, or any other vertebrate model. If so, then the use of data from life-time exposure/grow-out protocol to assess juvenile cancer risk may provide misleading results, and the reverse would also be true. It is possible, for instance, that the lack of proportionality in tumor response seen at ultra-low DBP dose in this study might reflect a time-dose interaction, in which tumors elicited at low dose grow more slowly than those at high dose. Under this circumstance, non-linearity in dose-response would be an inherent function of our juvenile termination protocol, and as such would be observed for all carcinogens eliciting hepatocellular carcinomas in this model. The most direct data we have on this question derives from our current ED_{001} study with aflatoxin B_1, using a treatment and grow-out protocol identical to that used for DBP. Two of the four independent trials are now completed, and the initial results (34) indicate that AFB_1 at low dose elicits a dose-response function that is considerably less steep on a log-log scale than observed in DBP, but still greater than 1.0. If these initial results are confirmed at the end of the study, the degree of sublinearity in tumor response at ultra-low dose in the trout model is determined by the carcinogen, and not the protocol.

Threshold tumor responses

The data presented here demonstrate that hepatic tumor response was not in direct proportion to DBP dose, but fell increasingly below direct proportionality (slope 1.0 on log/log scale) with

decreasing DBP dose. The shapes of two of the fitted curves for liver (quadratic logit, linear probit) and one of the fitted curves for stomach (linear probit) display increasingly steep slopes with decreasing dose, and thus may be taken to suggest that a finite dose may be reached in which there would be no observable increase above background tumor rate (slope of infinity), that is, a threshold. Although these data are c*onsistent* with a threshold interpretation, even the use of over 30,000 animals did not provide *proof* that a threshold was reached, or would exist, in either target organ for this carcinogen in this model. Several recent studies have explored the existence of a threshold for carcinogenicity by genotoxic carcinogens (29,30,35–37). Fukushima et al. (35) examined the induction of DNA adducts, 8-OHdG damage, and aberrant crypt foci biomarkers in the colon of rats treated with 2-amino-1-methyl-6-imidazo[4,5-b] pyridine (PhIP). The study covered an exceptionally wide range of PhIP exposure, 0.001 to 400 ppm fed for 16 weeks, at which time ACF/colon were determined. Rats per treatment ranged from 61 to 244, and observed ACF/colon ranged from 0.3 +/− 0.7 in controls to 5.0 +/− 2.8 at highest dose. By graphical analysis on a semilog scale (log dose vs total ACF) the authors claim evidence for a threshold dose of PhIP of 50 ppm because doses below that did not produce ACF/Foci different from background by simple pair-wise Dunnet-test. However, with variances in biomarker response of this magnitude even 250 animals/group provides insufficient statistical power to assess carcinogen-related response down to a background level of 0.3 ACF/colon, and especially to demonstrate significant departure from linearity in the low dose-response range. (The present study, by comparison, required approximately 27,000 animals treated with zero, 0.45 ppm, or 1.27 ppm DBP for adequate statistical power to demonstrate departure from linearity). In particular, the inability of a Dunnet-test to differentiate between 0.3 +/−0.7 ACF/colon (n=240) at zero dose, and 0.4 +/−0.8 ACF/colon (n=212) at 10 ppm does not provide statistical proof that a threshold has been reached or even that the response is significantly non-linear -- with sufficiently few animals and sufficiently large variances and background, any dose-response study will arrive at an exposure dose that does not elicit a response differing significantly from control. In addition, the semi-logarithmic graphical analysis used by these authors and others (29) is biased toward appearance of a threshold owing to simple mathematical reasons (expanded dose scale and compressed incidence scale). The insensitivity of this scaling for differentiating zero and near-zero incidences at low dose means that even a true proportional dose-response data set, that fits a straight-line-through-the-origin model, will show an apparent threshold on a semi-log scale.

Fukushima et al. (36) reported no-observed-effect levels for induction of the glutathione-S-transferase placental form altered foci biomarker in rat liver by low doses of N-nitrosodiethylamine or 2-amino-3,8-dimethylimidazo[4,5-f]quinoxaline. In this case as well, absence of background correction, variability in response, and limitation in animal numbers mitigate against a robust test of low-dose linearity for either carcinogen. In addition, this model as well as that reported by Williams et al. (37) used a protocol in which carcinogen treatment was followed by extended promotion by phenobarbital. At present, risk assessment models for carcinogenesis consider response to a single agent alone and the influence of a non-genotoxic promoter on the linearity of carcinogen response was not investigated in these studies. Such two-factor exposure protocols will require more intensive dose-dose-response study if we are to understand the interactions of carcinogen and promoter dose on biomarker or tumor response at low exposures and incidences pertinent to human cancer risk assessment.

Supplementary Material

Refer to Web version on PubMed Central for supplementary material.

Acknowledgments

We thank Dan Arbogast, Greg Gonnerman, Shiela Cleveland, Eric Johnson, Chance McDonald, Pat Loveland, Kate Mathews, Margaret Pratt, and Melissa Haendel for their assistance. This work was supported by National Institutes of Health Grants ES07060, ES03850, ES00210, ES04766, ES11267, and ES013534.

References

1. U.S. EPA. Proposed guidelines for carcinogen risk assessment. Washington, DC: 2006. p. 17960-18011.Fed. Reg. 61
2. Peto R, Gray R, Brantom P, Grasso P. Effects on 4080 rats of chronic ingestion of N-nitrosodiethylamine or N-nitrosodimethylamine: a detailed dose-response study. Cancer Res 1991;51:6415–6451. [PubMed: 1933906]
3. Swenberg JA, Hoel DG, Magee PN. Mechanistic and statistical insight into the large carcinogenesis bioassays on N-nitrosodiethylamine and N-nitrosodimethylamine. Cancer Res 1991;51:6409–6414. [PubMed: 1933905]
4. Poirier MC, Fullerton NF, Kinouchi T, Smith BA, Beland FA. Comparison between DNA adduct formation and tumorigenesis in livers and bladders of mice chronically fed 2-acetylaminofluorene. Carcinogenesis 1991;12:895–900. [PubMed: 2029755]
5. Williams DE, Bailey GS, Reddy A, Hendricks JD, Oganesian A, Orner GA, Pereira CB, Swenberg JA. The rainbow trout (Oncorhynchus mykiss) tumor model: recent applications in low-dose exposures to tumor initiators and promoters. Toxicol Pathol 2003;31:58–61. [PubMed: 12597433]
6. Bailey GS, Williams DE, Hendricks JD. Fish models for environmental carcinogenesis: the rainbow trout. Environ. Hlth. Persp 1996;104:5–21.
7. Bailey GS, Hendricks JD, Shelton DW, Nixon JE, Pawlowski N. Enhancement of carcinogenesis by the natural anticarcinogen indole-3-carbinol. J. Natl. Cancer Instit 1987;78:931–934.
8. Swenberg JA, Fryar-Tita E, Jeong YC, Boysen G, Starr T, Walker VE, Albertini RJ. Biomarkers in toxicology and risk assessment: informing critical dose-response relationships. Chem Res Toxicol 2008;21:253–265. [PubMed: 18161944]
9. Au WW. Usefulness of biomarkers in population studies: from exposure to susceptibility and to prediction of cancer. Int J Hyg Environ Health 2007;210:239–246. [PubMed: 17174154]
10. Nioi P, Pardo ID, Sherratt PJ, Snyder RD. Prediction of non-genotoxic carcinogenesis in rats using changes in gene expression following acute dosing. Chem Biol Interact 2008;172:206–215. [PubMed: 18328469]
11. Cavalieri EL, Higginbotham S, RamaKrishna NV, Devanesan PD, Todorovic R, Rogan EG, Salmasi S. Comparative dose-response tumorigenicity studies of dibenzo[alpha,l]pyrene versus 7,12-dimethylbenz[alpha]anthracene, benzo[alpha]pyrene and two dibenzo[alpha,l]pyrene dihydrodiols in mouse skin and rat mammary gland. Carcinogenesis 1991;12:1939–1944. [PubMed: 1934274]
12. Higginbotham S, RamaKrishna NV, Johansson SL, Rogan EG, Cavalieri EL. Tumor-initiating activity and carcinogenicity of dibenzo[a,l]pyrene versus 7,12-dimethylbenz[a]anthracene and benzo [a]pyrene at low doses in mouse skin. Carcinogenesis 1993;14:875–878. [PubMed: 8504480]
13. Prahalad AK, Ross JA, Nelson GB, Roop BC, King LC, Nesnow S, Mass MJ. Dibenzo[a,l]pyrene-induced DNA adduction, tumorigenicity, and Ki-ras oncogene mutations in strain A/J mouse lung. Carcinogenesis 1997;18:1955–1963. [PubMed: 9364006]
14. Reddy AP, Harttig U, Barth MC, Baird WM, Schimerlik M, Hendricks JD, Bailey GS. Inhibition of dibenzo[a,l]pyrene-induced multi-organ carcinogenesis by dietary chlorophyllin in rainbow trout. Carcinogenesis 1999;20:1919–1926. [PubMed: 10506105]
15. Yu Z, Loehr CV, Fischer KA, Louderback MA, Krueger SK, Dashwood RH, Kerkvliet NI, Pereira CB, Jennings-Gee JE, Dance ST, Miller MS, Bailey GS, Williams DE. In utero exposure of mice to dibenzo[a,l]pyrene produces lymphoma in the offspring: role of the aryl hydrocarbon receptor. Cancer Res 2006;66:755–762. [PubMed: 16424006]
16. Reddy AP, Spitsbergen JM, Mathews C, Hendricks JD, Bailey GS. Experimental hepatic tumorigenicity by environmental hydrocarbon dibenzo[a,l]pyrene. J Environ Pathol Toxicol Oncol 1999;18:261–269. [PubMed: 15281236]

17. Mumford JL, Cooke M. Indoor air sampling and mutagenicity studies of emissions from unvented coal combustion. Environ Sci Technol 1987;21:308–311.
18. Kozin IS, Gooijer C, Velthorst NH. Direct determination of dibenzo[a,l]pyrene in crude extracts of environmental samples by laser-excited Shpol'skii spectroscopy. Anal. Chem 1995;67:1623–1626.
19. Snook ME, Severson RF, Arrendale RF, Higman HC, Chortyk OT. The identification of high molecular weight polynuclear aromatic hydrocarbons in a biologically active fraction of cigarette smoke condensate. Beitr. Tabakforsch 1977;9:79–101.
20. Lee, BC.; Hendricks, JD.; Bailey, GS. Toxicity of mycotoxins in the feed of fish. In: Smith, JE.; Henderson, RS., editors. Mycotoxins and Animal Foods. Boca Raton, FL: CRC Press; 1991. p. 607-626.
21. Loveland PM, Reddy AP, Pereira CB, Field JA, Bailey GS. Application of matrix solid-phase dispersion in the determination of dibenzo[a,l]pyrene content of experimental animal diets used in a large-scale tumor study. J Chromatogr A 2001;932:33–41. [PubMed: 11695866]
22. Hendricks JD, Meyers TR, Shelton DW. Histological progression of hepatic neoplasia in rainbow trout (*Salmo gairdneri*). Natl. Cancer Inst. Monogr 1984;65:321–336. [PubMed: 6087143]
23. Dashwood RH, Arbogast DN, Fong AT, Pereira C, Hendricks JD, Bailey GS. Quantitative inter-relationships between aflatoxin B1 carcinogen dose, indole-3-carbinol anti-carcinogen dose, target organ DNA adduction and final tumor response. Carcinogenesis 1989;10:175–181. [PubMed: 2491968]
24. Harttig U, Bailey GS. Chemoprotection by natural chlorophylls in vivo: inhibition of dibenzo[a,l] pyrene-DNA adducts in rainbow trout liver. Carcinogenesis 1998;19:1323–1326. [PubMed: 9683196]
25. Pratt MM, Reddy AP, Hendricks JD, Pereira C, Kensler TW, Bailey GS. The importance of carcinogen dose in chemoprevention studies: quantitative interrelationships between, dibenzo[a,l]pyrene dose, chlorophyllin dose, target organ DNA adduct biomarkers and final tumor outcome. Carcinogenesis 2007;28:611–624. [PubMed: 16973675]
26. Van Ryzin J, Rai K. A dose-response model incorporating nonlinear kinetics. Biometrics 1987;43:95–105. [PubMed: 3567309]
27. EPA. Benchmark Dose Software. 2008.
28. Fong AT, Dashwood RH, Cheng R, Mathews C, Ford B, Hendricks JD, Bailey,9 GS. Carcinogenicity, metabolism and Ki-ras proto-oncogene activation by 7,12-dimethylbenz[a]anthracene in rainbow trout embryos. Carcinogenesis 1993;14:629–635. [PubMed: 8472326]
29. Waddell WJ. Thresholds of carcinogenicity in the ED01 study. Toxicol Sci 2003;72:158–163. [PubMed: 12604845]
30. Crump KS, Clewell HJ. Evidence of a "clear and consistent threshold" for bladder and liver cancer in the large ED01 carcinogenicity study. Toxicol Sci 2003;74(485):485–486. [PubMed: 12730607] author reply
31. Calabrese EJ, Baldwin LKA. The frequency of U-shaped dose-responses in the toxicology literature. Toxicological Sciences 2001;62:330–338. [PubMed: 11452146]
32. Poirier MC, Beland FA. DNA adduct measurements and tumor incidence during chronic carcinogen exposure in rodents. Environmental Health Perspectives 1994;102:161–165. [PubMed: 7889840]
33. Driver HE, White INH, Butler WH. Dose-response relationships in chemical carcinogenesis: Renal mesenchymal tumors in the rat by single dose dimethynitrosamine. Br. J. Exp. Pathol 1987;68:133–143. [PubMed: 3580278]
34. Williams DE, Orner G, Willard KD, Tilton S, Hendricks JD, Pereira C, Benninghoff AD, Bailey GS. Rainbow trout (*Oncorhynchus mykiss*) and ultra-low dose cancer studies. Comparative Biochem. Physiol. Part C 2009;149:175–181.
35. Fukushima S, Wanibuchi H, Morimura K, Iwai S, Nakae D, Kishida H, Tsuda H, Uehara N, Imaida K, Shirai T, Tatematsu M, Tsukamoto T, Hirose M, Furukawa F. Existence of a threshold for induction of aberrant crypt foci in the rat colon with low doses of 2-amino-1-methyl-6-phenolimidazo [4,5-b]pyridine. Toxicol Sci 2004;80:109–114. [PubMed: 15014208]
36. Fukushima S, Wanibuchi H, Morimura K, Wei M, Nakae D, Konishi Y, Tsuda H, Uehara N, Imaida K, Shirai T, Tatematsu M, Tsukamoto T, Hirose M, Furukawa F, Wakabayashi K, Totsuka Y. Lack of a dose-response relationship for carcinogenicity in the rat liver with low doses of 2-amino-3,8-

dimethylimidazo[4,5-f]quinoxaline or N-nitrosodiethylamine. Jpn J Cancer Res 2002;93:1076–1082. [PubMed: 12417036]

37. Williams GM, Iatropoulos MJ, Wang CX, Jeffrey AM, Thompson S, Pittman B, Palasch M, Gebhardt R. Nonlinearities in 2-acetylaminofluorene exposure responses for genotoxic and epigenetic effects leading to initiation of carcinogenesis in rat liver. Toxicol Sci 1998;45:152–161. [PubMed: 9848122]

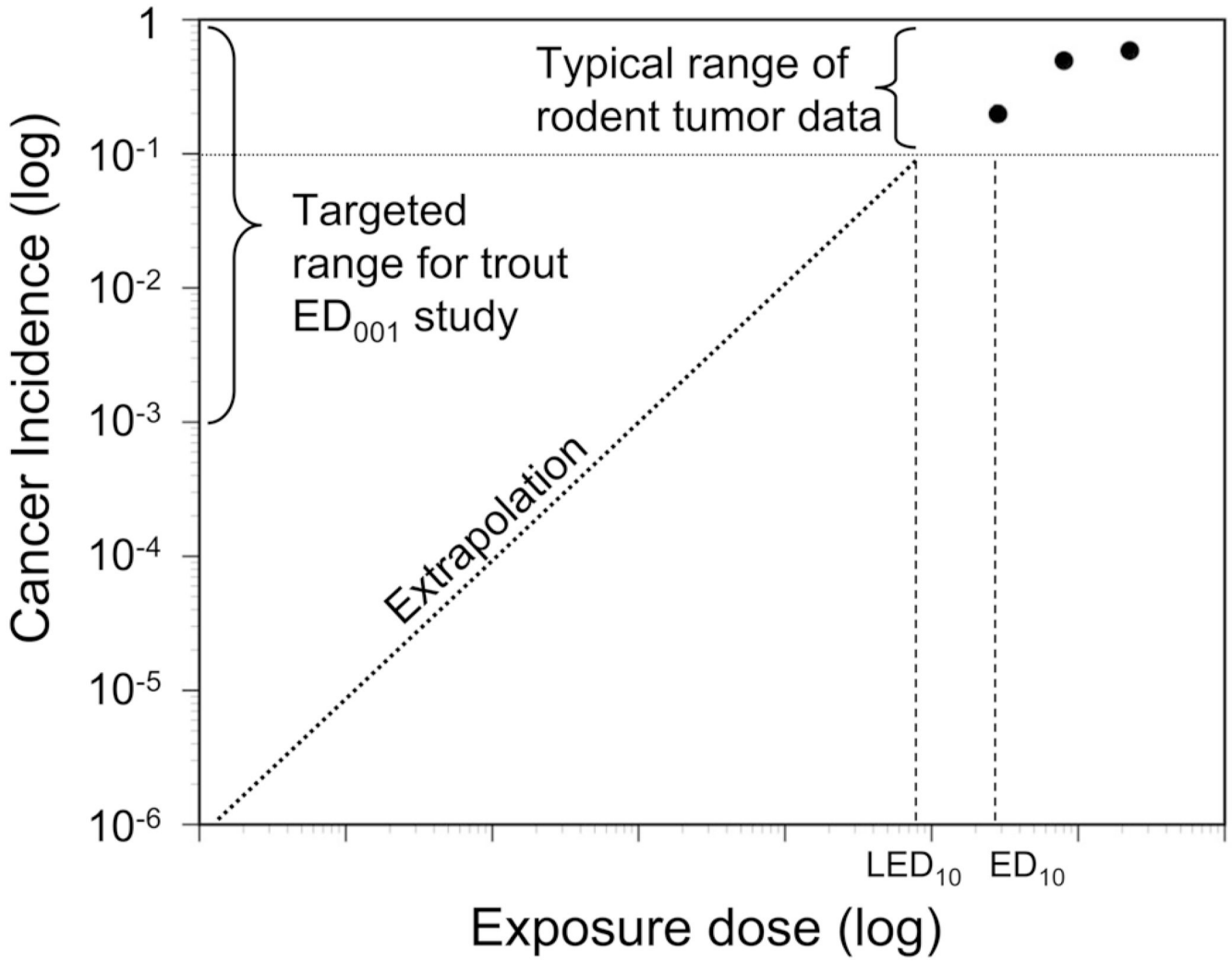

Figure 1.
Hypothetical illustration of the magnitude of extrapolation necessary to evaluate acceptable human exposure based on typical rodent bioassay data, and the design goal of the present studies to extend the range of available tumor data. Typical rodent bioassay data range from approximately 10% incidence upward towards 100%, whereas the ED_{001} experiments in this report were designed to seek tumor data down at least two additional orders of magnitude, to 0.1% incidence.

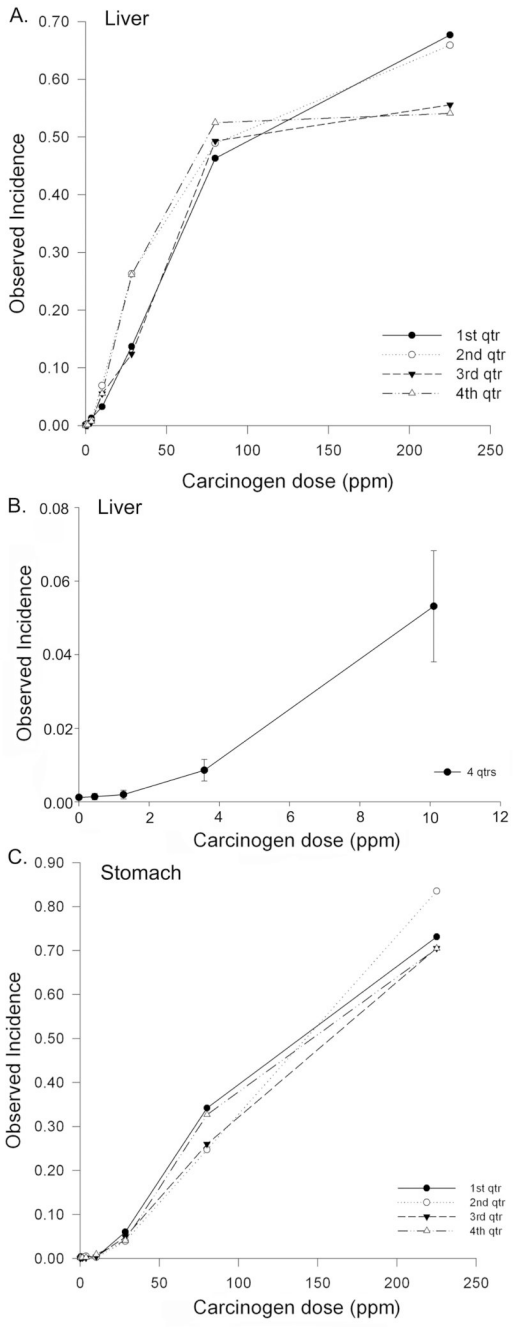

Figure 2.

Incidence of liver and stomach neoplasia versus carcinogen dose. (A) Liver tumor incidence with each quartile shown separately. Each data point represents mean incidence among replicates at that dose, and each line represents one of four independent dose-response experiments. (B) Overall trend in liver tumor incidence for the 5 lowest doses (simple mean and standard deviation for the 4 quartiles). (C) Stomach tumor incidence with each quartile shown separately as in A.

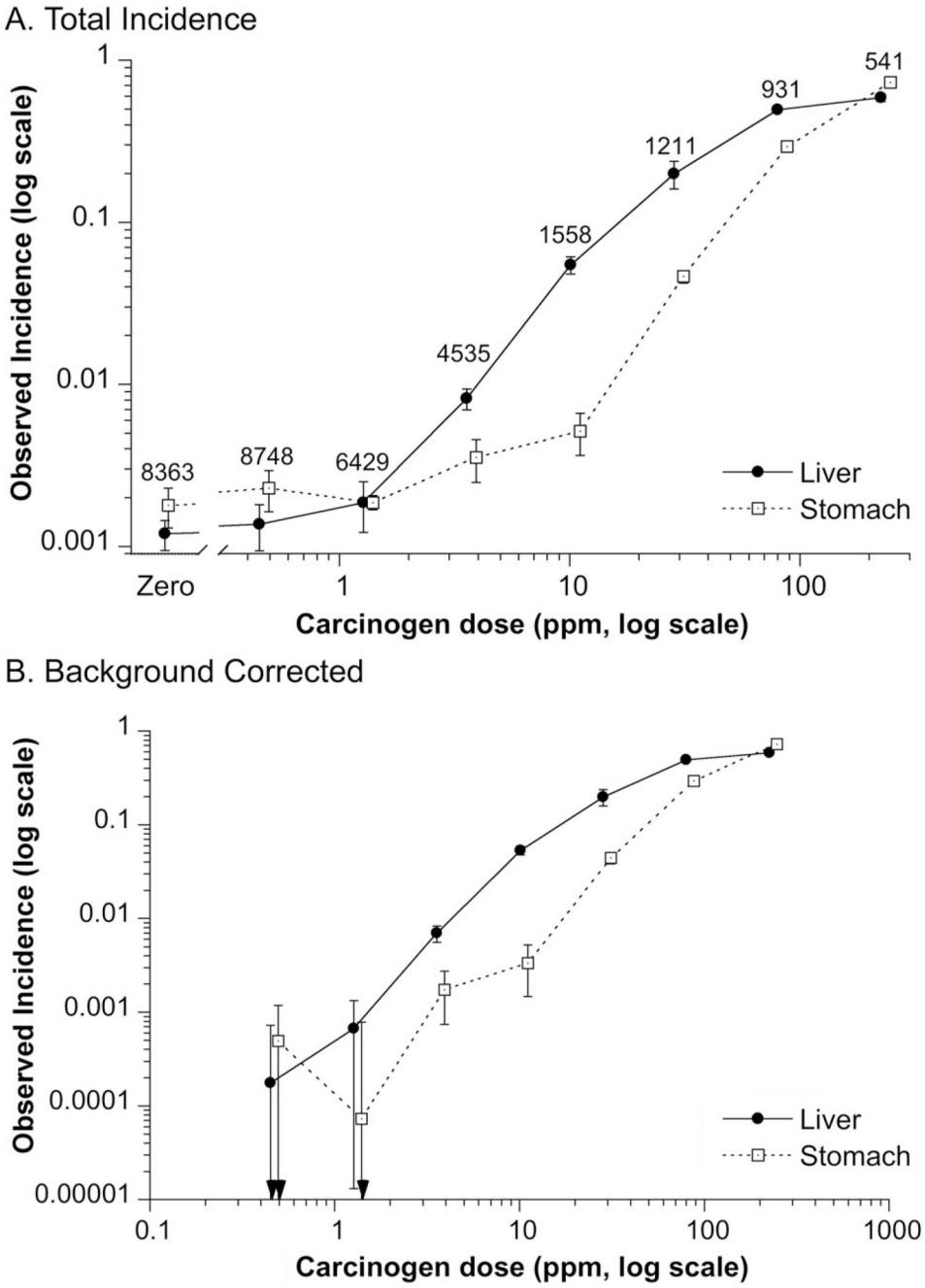

Figure 3.

Incidence of liver and stomach neoplasia versus carcinogen dose plotted on a log scale with four quartiles combined (A) without background correction and (B) corrected for the combined background incidence. Error bars are standard error (SE) (see Statistical Methods) and the number of animals per treatment group is shown above the symbols in 3A.

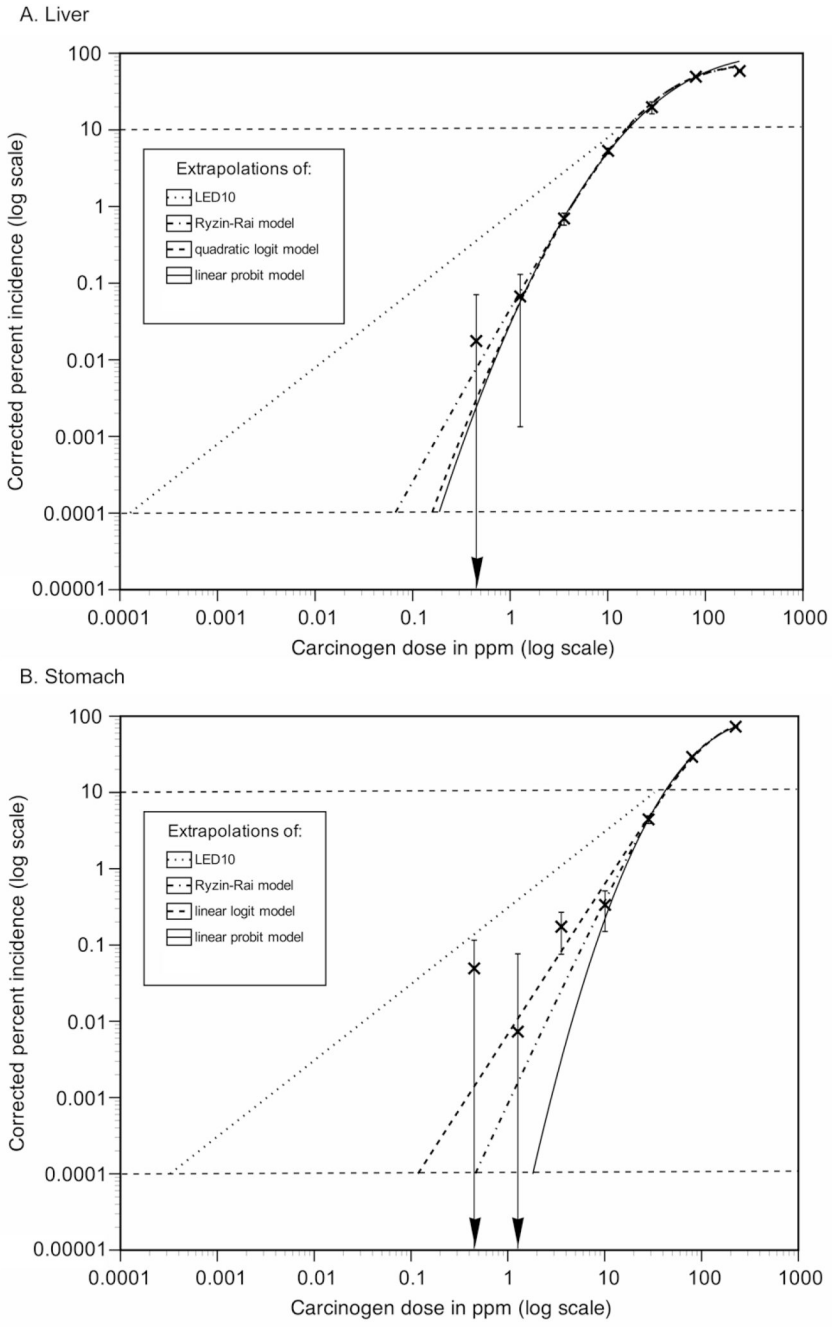

Figure 4.

Extrapolations of the dose-response portion from well-fitting models for trout tumor incidence data and from LED_{10} lines. The dotted lines represent default linear extrapolations from LED_{10} points of departure, which were established using a standard linear logit model fit to the incidences from the highest three doses (after excluding the highest dose, 225, for liver). Points (Xs) are observed pooled incidences corrected for the pooled observed background with approximate SE bars for the corrected incidences (see Statistical Methods). (A) Three models that fit the liver data well are quadratic logit (3 dose-response parameters, dashed line), Ryzin-Rai (3 dose-response parameters, alternating dotted and dashed line) and the linear probit (2 dose-response parameters, solid line). (B) Three models that fit the stomach data well are the

linear logit (2 dose-response parameters), linear probit (2 dose-response parameters) and the Ryzin-Rai (3 dose-response parameters).

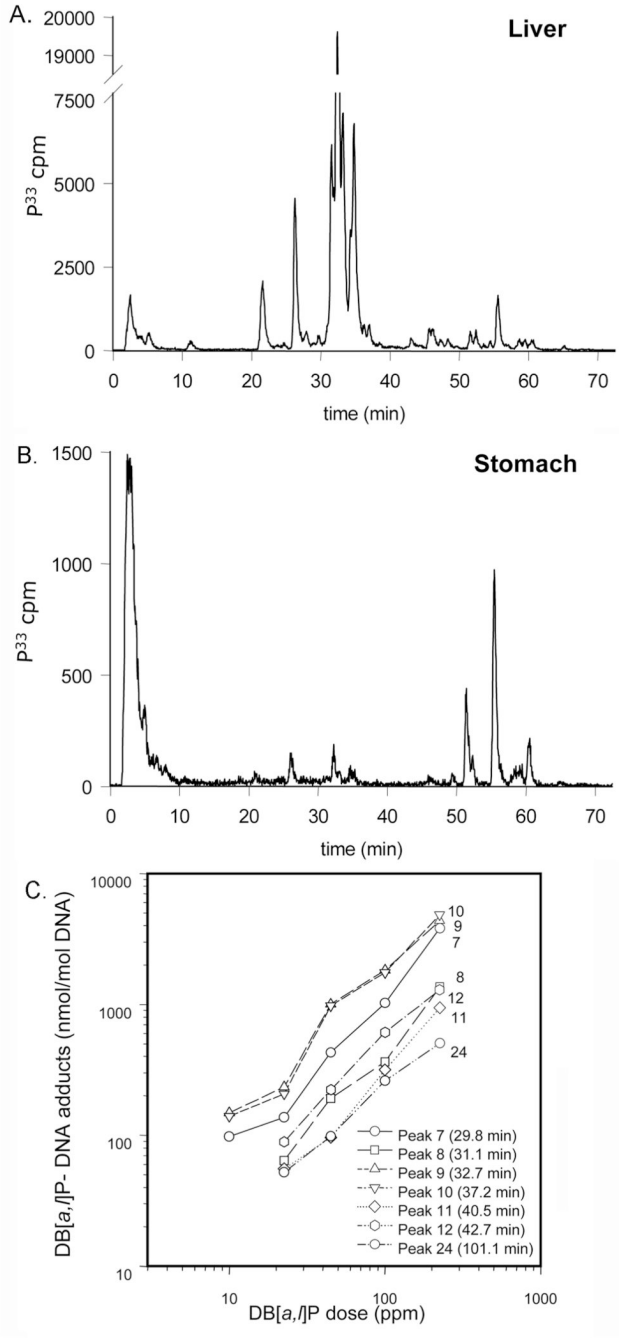

Figure 5.

DBP-DNA adducts from rainbow trout after ^{33}P-postlabeling/HPLC analysis. Trout were sampled on day 29 after 28 days of dietary DBP treatment. Each sample represents 3 pools of 5 livers or stomachs. A. Representative liver DNA adduct profile. B. Representative stomach DNA adduct profile. C. Dose-response of seven major hepatic DNA adduct peaks.

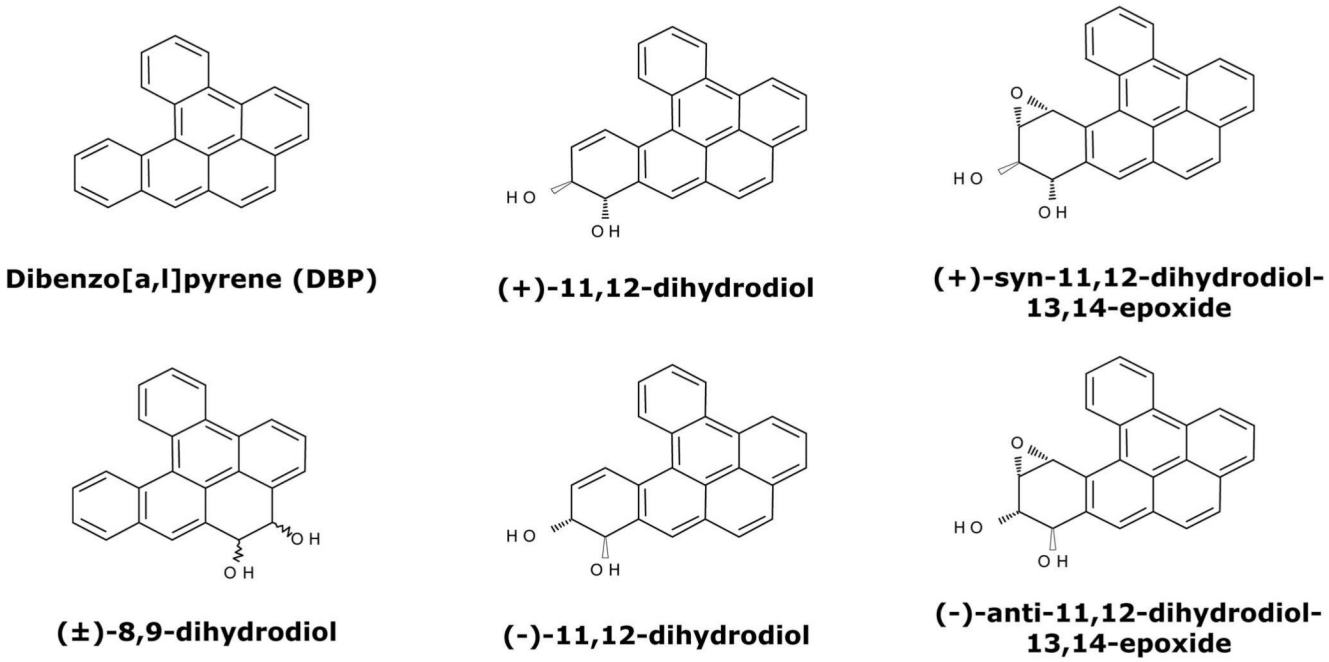

Figure 6.
Structures of DBP and potential intermediate metabolites.

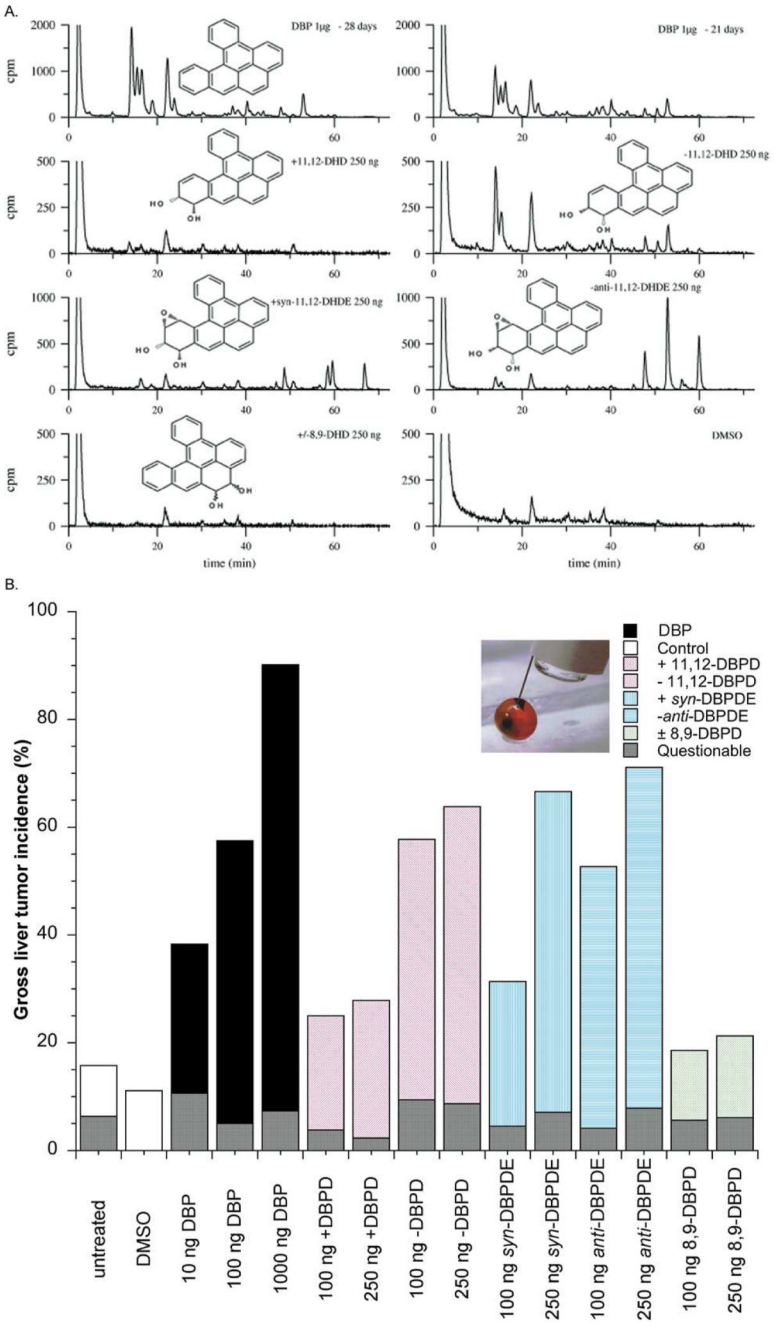

Figure 7.

Effects of DBP metabolites on DNA adduct profiles and comparative carcinogenic potency. (A) Comparison of hepatic DBP-DNA adducts generated by microinjection of DBP and metabolites into trout embryos. (B) Comparison of hepatic tumorigenicity of DBP and metabolites by trout embryo microinjection.

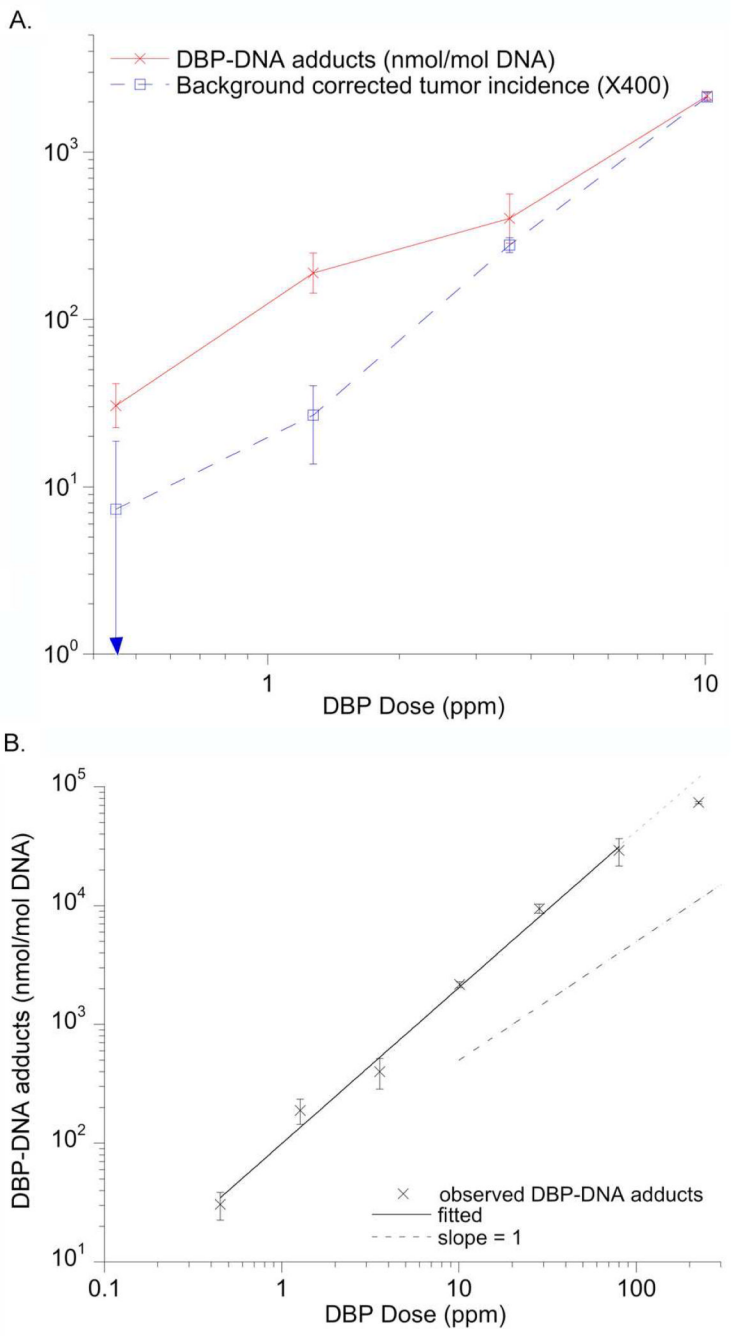

Figure 8.

Dose-response for total DBP-DNA adduction in trout liver. (A) A comparison of the observed (unmodeled) dose responses for DBP-DNA adduct accumulation and liver tumor incidence at low DBP exposures. The adduct and incidence data were approximately normalized to the 10.1 ppm DBP dose point by multiplying the observed incidences by a factor of 400. (B) Dose-response for DNA adduct accumulation at all DBP doses, modeled on the log-log scale. Total genomic DNA was purified from pooled livers each, taken on day 29 after 28 days of DBP treatment. Sample size per DBP dose are N=4 pools of five livers each except at the two lowest doses (N=2 and 3 at DBP dose = 0.45 and 1.27 ppm). Data points represent means +/− SE, with total adducts quantified by ^{32}P-TLC postlabeling.

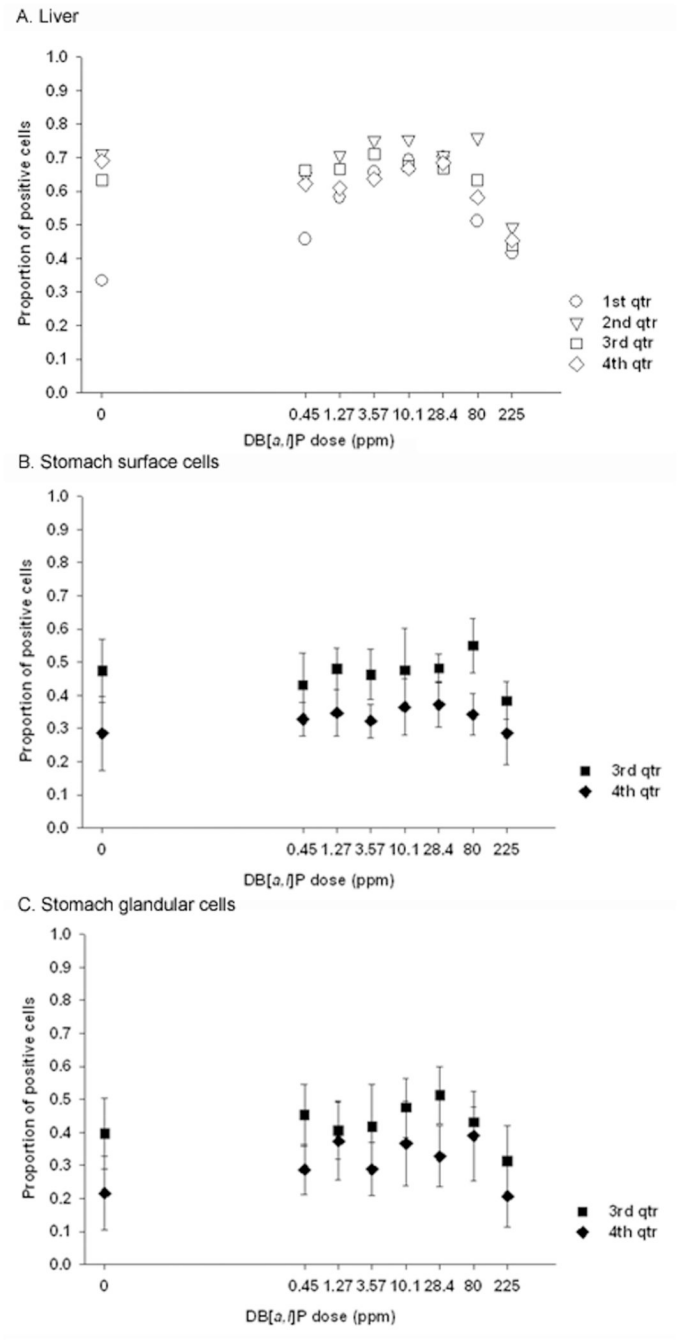

Figure 9.

Cell proliferation in (A) hepatocytes, (B) stomach surface cells, and (C) stomach glandular cells versus carcinogen dose. Five fish per dose per quartile (liver, all 4 quartiles: stomach, quartiles 3 and 4) were sampled for cell proliferation 2 (not shown) and 4 weeks following treatment with DBP. A minimum of 1000 cells were counted from each tissue per fish to obtain the proportion of positively stained cells. Each datapoint represents the mean of 5 fish.

Table 1

Experimental design. Tumor incidence is summarized by dose and quartile. A complete dataset at the tank level is included in the supporting information (Table S-1).

Experiment quarter	DBP dose (ppm diet)	Replicate groups necropsied	Animals necropsied	Histological liver neoplasia	Incidence	Stomach neoplasia	Incidence
1	0	23	2097	2	0.00095	5	0.00236
2	0	22	2056	4	0.00195	5	0.00236
3	0	25	2348	2	0.00085	1	0.00043
4	0	21	1862	2	0.00107	4	0.00200
1	0.45	24	2139	1	0.00047	9	0.00420
2	0.45	22	2021	4	0.00198	3	0.00148
3	0.45	25	2380	2	0.00084	5	0.00210
4	0.45	25	2208	5	0.00226	3	0.00136
1	1.27	14	1280	4	0.00313	2	0.00138
2	1.27	18	1672	5	0.00299	4	0.00234
3	1.27	19	1814	1	0.00055	3	0.00165
4	1.27	19	1663	2	0.00120	3	0.00180
1	3.57	8	737	9	0.01221	4	0.00513
2	3.57	14	1253	11	0.00878	7	0.00559
3	3.57	14	1327	8	0.00603	2	0.00151
4	3.57	14	1218	9	0.00739	3	0.00246
1	10.1	3	275	9	0.03273	1	0.00364
2	10.1	4	361	25	0.06925	1	0.00277
3	10.1	5	488	27	0.05533	2	0.00410
4	10.1	5	434	24	0.05530	4	0.00922
1	28.4	2	182	25	0.13736	11	0.06044
2	28.4	3	278	73	0.26259	11	0.03957
3	28.4	4	387	48	0.12403	19	0.04909
4	28.4	4	364	95	0.26099	15	0.04121
1	80	2	190	88	0.46316	65	0.342
2	80	2	186	91	0.48925	46	0.247
3	80	3	292	144	0.49315	76	0.260
4	80	3	263	138	0.52471	86	0.327
1	225	1	93	63	0.67742	68	0.731
2	225	1	85	56	0.65882	71	0.835
3	225	2	180	100	0.55556	127	0.706
4	225	2	183	99	0.54098	129	0.705

Extrapolated doses to cause one excess tumor in a million individuals according to selected models.

Extrapolation Type	Extrapolated dose (ppb) causing 0.0001 percent incidence[1]		Ratio (Model over LED_{10})	
	Liver	Stomach	Liver	Stomach
Example of an LED_{10}	0.126[2]	0.326[3]		
Example of an ED_{10}	0.155[2]	0.387[3]	1.23	1.19
Probit linear in log dose	186	1813	1480	5560
Logit type model	158[4]	120[5]	1250	364
Ryzin-Rai model	66	460	524	1390

[1] 0.0001 percent incidence = 0.000001 (proportion) incidence = 1 in one million

[2] Example based on data for DBP doses 28.4 and 80 (observed incidence greater than 10%) using logit linear in log dose model. The LED_{10} was calculated using binomial error (because accounting for overdispersion at DBP dose 28.4 would have shrunk, and therefore penalized, the LED_{10}).

[3] Example based on data for DBP doses 80 and 225 (observed incidence greater than 10%) using logit linear in log dose model with binomial error.

[4] Logit quadratic in log dose because linear gave poor fit (see results).

[5] Logit linear in log dose.

Ki-*ras* mutation spectrum in liver (A) and stomach (B) of trout from DBP ED_{001} experiment.

A. Liver													
DBP dose (ppm)	**# tumors examined**	**# (%) mutations**	**Codon 12**				**Codon 13**		**Codon 61**				**Double**
			(1)G/A	**(1)G/C**	**(2)G/T**	**(2)G/A)**	**(1)G/C**	**(2)G/T**	**(2)A/T**	**(2)A/T**	**(3)G/T**	**(3)G/C**	
0	5	3 (60)	2	1									
0.45	4	4 (100)	1	1	1							1	
1.27	5	3 (60)	1			1						1	
3.57	10	8 (80)	3		2		1		1				1
10.1	20	19 (95)	8	1	4		3	1					2
28.4	38	32 (84)	15	3	7		1		1	1	2		2
80	40	36 (90)	10	3	14			3	2	1		3	
225	34	28 (82)	4	6	6		3		5	1			3

B. Stomach							
DBP dose (ppm)	**# tumors examined**	**# (%) mutations**	**Codon 12**	**Codon 13**	**Codon 61**		
			(1)G/A	**(1)G/C**	**(2)A/T**	**(2)A/G**	**(3)G/T**
0	7	4 (57)	2	1		1	
0.45	10	4 (40)			1	3	
1.27	6	2 (33)			2		
80	39	29 (74)			28		1
225	28	10 (36)			10		